



Published in final edited form as:

*Prog Pediatr Cardiol.* 2010 August 1; 29(2): 79–85. doi:10.1016/j.ppedcard.2010.06.011.

## Effects of congenital heart disease on brain development

Patrick S. McQuillen<sup>a,\*</sup>, Donna A. Goff<sup>b</sup>, and Daniel J. Licht<sup>c</sup>

<sup>a</sup> Department of Pediatrics, Division of Critical Care, University of California, San Francisco, CA, United States

<sup>b</sup> Department of Pediatrics, Division of Cardiology, Children's Hospital of Philadelphia, Philadelphia, PA, United States

<sup>c</sup> Department of Pediatrics, Division of Neurology, Children's Hospital of Philadelphia, Philadelphia, PA, United States

### Abstract

Brain and heart development occurs simultaneously in the fetus with congenital heart disease. Early morphogenetic programs in each organ share common genetic pathways. Brain development occurs across a more protracted time-course with striking brain growth and activity-dependent formation and refinement of connections in the third trimester. This development is associated with increased metabolic activity and the brain is dependent upon the heart for oxygen and nutrient delivery. Congenital heart disease leads to derangements of fetal blood flow that result in impaired brain growth and development that can be measured with advanced magnetic resonance imaging. Delayed development results in a unique vulnerability to cerebral white matter injury in newborns with congenital heart disease. Delayed brain development and acquired white matter injury may underlay mild but pervasive neurodevelopmental impairment commonly observed in children following neonatal congenital heart surgery.

### Keywords

Congenital heart defects; Brain development; White matter injury; Periventricular leukomalacia; Infant heart surgery; Fetal circulation

## 1. Introduction

Despite established mechanisms that preserve brain oxygen and nutrient delivery, newborns with certain forms of congenital heart disease are born with smaller head circumferences possibly indicating impaired brain growth [1]. Somatic and brain growth patterns vary by type of congenital heart disease. Newborns with hypoplastic left heart syndrome (HLHS) are smaller in all dimensions, but head volume is disproportionately decreased. In a recent study, ascending aortic diameter predicted the degree of microcephaly in newborns with HLHS [2]. Hypoplasia or atresia of the ascending aorta limits antegrade cerebral blood flow and thus brain blood flow must arise from the ductus arteriosus in a retrograde fashion across the aortic isthmus. In comparison, infants with isolated aortic coarctation have a greater head circumference relative to birth weight, as flow to the head and neck vessels is unobstructed while blood flow in the descending aorta may be compromised. The relationship between amount of antegrade flow in the ascending aorta and brain growth fails to describe why newborns with d-transposition of the great arteries (d-TGA) have smaller head circumferences with a normal birth weight. d-

\*Corresponding author. mcquillp@peds.ucsf.edu (P.S. McQuillen), GOFFD@email.chop.edu (D.A. Goff).

TGA growth patterns suggest that blood flow alone does not completely describe the connection between heart and brain development.

Brain and heart development intersect at many levels. Early brain and heart organogenesis occur simultaneously in the human fetus and invoke similar developmental programs including stem and progenitor cell proliferation, cell fate commitment, migration, left/right and dorsal/ventral patterning [3–5]. At later stages, after completion of gross morphological development in both organs, brain development continues with a dramatic increase in brain size (Fig. 1) due to elaboration of neuronal microstructure (e.g. dendrites, axons and synapses) and the onset of myelination. The formation and refinement of connections in the brain requires neuronal activity, leading to an increase in brain metabolism with dependence upon heart function for oxygen and substrate delivery.

## 2. Shared genetic pathways in early brain and heart development

Similar morphogenetic events in brain and heart development engage many of the same genes including: sonic hedgehog (progenitor proliferation), notch, jagged, Nkx2.5 (cell fate commitment), fibroblast growth factor-8, nodal, lefty1 (left/right asymmetry), transforming growth factor beta, and retinoic acid (ventral patterning). It has long been recognized that many forms of syndromic congenital heart disease (e.g. Down's, DiGeorge, Noonan, and Williams–Beuren) include neurodevelopmental impairment. However, the involvement of shared genetic pathways in heart and brain development suggests that subtle neurodevelopmental abnormalities may occur in non-syndromic congenital heart disease.

Formation of the human heart occurs during the first postconceptual days to weeks, with formation of the first and second heart fields by day 15 and rhythmic contractions of a primitive tube beginning by embryonic day 21. Rightward looping, outflow tract formation and septation result in a morphologically mature heart formed by day 50, or gestational week 7 (GW7) (reviewed in Srivastava, 2006 [3]). The majority of cardiac tissue forms from lateral plate mesoderm in response to signals emanating from adjacent endoderm. Neural crest tissue, derived from ectoderm, contributes to both the brain and heart.

Brain tissue arises entirely from ectoderm. In the brain, the primitive neural tube forms slightly later, by GW5, than the cardiac crescent. Radial glia, the neural stem cells, are identifiable at this time [6]. Dorsal ventral patterning (sonic hedgehog), establishes distinct domains throughout the neuraxis, while rostral caudal patterning subdivides the developing forebrain. Formation of the cerebral cortex occurs from GW7 through GW18 with proliferation of neurons in the ventricular and subventricular zones surrounding the cerebral ventricles [7]. While the heart is morphologically mature by GW7, brain development extends over a much longer time period, with distinct morphologic events (e.g. cell proliferation, migration, axon pathfinding and target selection) occurring in the first two trimesters, [8] followed by a prolonged period of activity-dependent refinement of connections that occurs in the third trimester and into postnatal life. Excitatory projection neurons migrate radially into specific neocortical layers, while inhibitory interneurons migrate tangentially from the ganglionic eminence. A mature six-layered cortex does not appear until GW26 [9]. Following corticogenesis, central nervous system neurons must form connections through axon outgrowth, pathfinding, target selection and innervation. Formation of connections between thalamus and cortex requires a transient population of early born neurons, referred to as subplate neurons because of their location as a discrete layer below the cortical plate (reviewed in McQuillen [10]). In the human fetus, thalamocortical pathfinding takes place between the histological emergence of the subplate at the end of the first trimester [11] and the appearance of cholinesterase positive fibers in the subplate at GW17–20 [12]. Thalamocortical fibers accumulate during a ‘waiting period’ from GW17 [11,12] through GW22–26 [12,13] before innervating the cortical plate.

### 3. Activity-dependent brain development

Gross morphologic events of brain development are completed by the end of the second trimester. The third trimester involves a period of dramatic brain growth and refinement of connections that is dependent upon endogenous, spontaneous neuronal activity arising at multiple levels [14]. In the visual system, this endogenous activity takes the form of spontaneous waves of neuronal activation that sweep across and tile the retina and are transmitted to thalamus and cortex. Patterned activity sculpts developing neural circuits into mature, precise patterns [15]. Ocular dominance columns in the visual system are a representative example of such a patterned circuit. Ocular dominance columns represent non-overlapping eye-specific innervation to primary visual cortex and form the basis of binocular vision. In higher primates, ocular dominance columns have fully formed by birth before onset of visually driven activity [16,17]. While all major brain structures have formed by the 2nd trimester, during the third trimester cortical development continues with development of secondary and tertiary gyri (Fig. 1) [8].

### 4. White matter maturation

At a cellular level, this brain growth involves the elaboration of dendritic arbors and formation of neuronal connections. Myelination of neuronal axons also begins during this period, with a characteristic caudal to cranial pattern [18]. By the end of the third trimester, myelination extends to the posterior limb of the internal capsule and involves the motor fibers of the pyramidal tract. In neocortex, myelination begins in the optic radiations and occipital white matter soon after birth [19]. Oligodendrocytes (OL) are glial cells responsible for laying down myelin on neuronal axons. The maturation of the OL lineage has been characterized in detail and consists of four primary stages; OL progenitor, pre OL, immature OL and mature OL. Each stage is uniquely identified by monoclonal antibodies to marker proteins expressed during differentiation. Pre-myelinating OL precursor cells, characterized by expression of OL1, OL4, Olig 2 and Sox 10, are present in their largest concentration in the periventricular white matter from about 23 weeks of gestational age to 34 weeks [20]. These pre-myelinating OL are very sensitive to oxidative stress injury which, in the presence of perturbations in cerebral blood flow, are the key ingredient to the formation of periventricular white matter injury in the form of periventricular leukomalacia (PVL) [21]. This maturation dependent vulnerability is supported by the observation that the white matter of a 7-day-old rat was more resilient to hypoxia-ischemia than a 2-day-old [22]. Experimentally, the maturation of pre-myelinating OL can be arrested in-vivo during this vulnerable stage by the use of hypoxic conditions such as might exist in utero for fetuses with severe CHD [23].

### 5. The effects of congenital heart disease on fetal brain oxygen delivery and growth

Fetal blood flow is unique in a number of respects that have distinct impact on cerebral blood flow. In the fetus, gas exchange occurs in the placenta with oxygenated blood returning through the umbilical vein and ductus venosus to the portal vein, inferior vena cava and right atrium and deoxygenated blood returning to the placenta via the umbilical artery (Fig. 2A). Prior to birth, blood flow to the lungs is very low due to elevated pulmonary vascular resistance and relatively low lung volumes. Two connections exist between the systemic and pulmonary circulations: the foramen ovale connecting the right and left atria and the ductus arteriosus between the pulmonary trunk and descending aorta. Umbilical venous blood is preferentially directed through the ductus venosus into the left lobe of the liver. As a consequence the oxygen saturation is higher in the left hepatic veins as they join the inferior vena cava (IVC) resulting in streams of blood with different saturations. The higher saturated stream containing blood from the ductus venosus is preferentially directed across the foramen ovale to the left atrium

(Fig. 2A). This blood mixes with the limited amount of pulmonary venous blood returning from the lungs, resulting in a saturation in the fetal left ventricle of ~65%. Blood ejected by the right ventricle consists of venous blood from the superior vena cava as well as the relatively desaturated streams from the inferior vena cava and coronary sinus. The resulting saturation in the fetal right ventricle is ~55%.

In two common forms of congenital heart disease, d-TGA and HLHS, alterations in fetal blood flow may lead to decreased brain oxygen delivery. In d-TGA, the aorta arises from the right ventricle and thus receives the relatively desaturated blood from the superior vena cava and lower saturation stream of blood in the inferior vena cava (Fig. 2). The higher saturated stream from the left hepatic veins is directed normally across the foramen ovale to the morphologic left ventricle. The left ventricle however is connected to the pulmonary trunk and this higher saturated blood (~65%) is delivered to the lungs and lower body (Fig. 2B). In HLHS, the fetal circulation is characterized by increased left atrial pressure, resulting in reversal of flow across the foramen ovale (Fig. 2C). Left ventricular filling is impaired and there is either no ventricular output or stroke volume is diminished with reduced or absent flow into the ascending aorta. All venous return mixes in the right ventricle and is ejected into the pulmonary trunk and ductus arteriosus (Fig. 2C). Although the resulting saturation is not as low as with d-TGA, a number of factors may restrict flow to the cerebral circulation. In many cases, flow to the head and neck vessels only occurs by retrograde flow into the transverse aorta (Fig. 2C).

## 6. Fetal ultrasound assessment of cerebral physiology

Blood flow to the fetal brain is estimated to be almost one quarter of the combined ventricular output in the third trimester [24]. Preferential blood flow to the brain is preserved through autoregulatory mechanisms during pathological states, such as placental insufficiency. This 'brain sparing' phenomenon results in relative preservation of head growth, despite somatic growth restriction [25–27]. Clinically, this fetal autoregulatory response can be assessed using Doppler ultrasound by insonating the middle cerebral artery (MCA) and measuring the pulsatility, or resistance indices (PI or RI, respectively) [28]. MCA PI is calculated using the equation: peak systolic–diastolic/mean, values being derived from the MCA waveform as shown in Fig. 3A [28]. Using these measures, an increased diastolic flow from decreased vascular resistance will result in a lower MCA PI. Typically, MCA PI decreases with increasing gestational age, presumed to be a result of increase cerebral metabolic demand or decreasing fetal PaO<sub>2</sub> [25,29,30]. Although a lower MCA PI or RI is reflective of decreased cerebrovascular resistance, the cerebroplacental ratio (CPR), a ratio of MCA to umbilical artery PI, is a better predictor of adverse perinatal outcome and poor growth [31]. A CPR ratio <1 is reflective of redistribution of blood flow towards the brain [28]. Alterations in cerebral blood flow (CBF) have been described in pregnancies complicated by intrauterine growth restriction (IUGR) [25,32] and in fetuses with complex congenital heart disease [33–35]. In fetuses with CHD, MCA PI waveforms demonstrate an increase in diastolic flow for hypoxemic fetuses (including d-TGA) compared to normal fetuses as shown in Fig. 3b [28,34,35]. Likewise, HLHS fetuses are also more likely to have a decrease in middle cerebral artery (MCA) pulsatility index [34,35], a decrease MCA RI and lower CPR ratio often being <1 compared to normal fetuses [33,36] Fig. 4. These MCA PI changes are presumed to be a result of limited or no antegrade aortic blood flow with dependency on retrograde flow from the ductus arteriosus to provide cerebral blood flow. In addition, HLHS fetuses also have impaired RV performance and lower cardiac output compounding the limitations in regulatory capacity and potentially influencing MCA PI [37]. These limitations may explain why after in utero aortic valvuloplasty fetuses showed no significant improvement in MCA PI or CPR ratio [36].

These alterations in cardiac output observed in utero may significantly influence cerebral blood flow (CBF) and may lead to altered ability to regulate CBF during the transitional period and

following surgery [38]. Although there is a compensatory “brain sparing” response in utero, there is likely a threshold that once reached results in altered brain growth and development.

## 7. Fetal brain MRI

The idea that delayed postnatal brain development results from disordered fetal cerebral blood flow suggests two predictions; 1) Delayed brain development should begin during fetal life; 2) Different forms of CHD should manifest different degrees of delayed development. Studies using fetal brain ultrasound have suggested that decline in head growth begins after mid-gestation in fetuses with HLHS [39]. Definitive evidence for delayed fetal brain development has recently been published for a cohort of fetuses with congenital heart disease [40]. In this study, brain volumes and proton  $^1\text{H}$ -MRS were compared among 55 fetuses with CHD compared with 50 normal fetuses between 25 and 37 gestational weeks. No differences were found between controls and CHD fetuses during the second trimester. During the third trimester, a progressive impairment of brain volumes was noted in fetuses with left-sided obstructive lesions. Fetuses with aortic atresia and no antegrade blood flow in the aortic arch had larger delays in the expected increase in NAA/Cho and greater impairment of growth in brain volume. These observations confirm that impaired brain development begins during fetal life due to impaired fetal cerebral blood flow, oxygen and substrate delivery and that compensatory mechanisms (brain sparing effect) are overwhelmed (Fig. 4).

## 8. Transitional circulation

The transition from fetal (placental) circulation to neonatal circulation is complex and requires maintenance of CBF during a period of a precipitous decline in pulmonary vascular resistance [41] along with an increase in systemic vascular resistance [42]. In neonates without congenital heart defects, these changes are facilitated by the closure of the ductus arteriosus, with consequent isolation of the pulmonary blood flow from systemic blood flow. In neonates with complex CHD, closure of the ductus may be catastrophic as a result of inadequate pulmonary or systemic blood flow and is prevented with intravenous administration of Prostaglandin E. This maintenance of ductal patency by PGE potentially compromises CBF by perpetuating shared blood flow between the pulmonary and systemic circulation particularly as the pulmonary vascular resistance drops. Although some data is available on how CBF is regulated during the transitional period in premature infants, little is known about the regulatory capacities of term neonates or neonates with congenital heart disease. In healthy premature infants, CBF gradually increases with time [43,44] with the greatest increase occurring in the first few days of life [45]. In premature and term infants with gestational ages between 32 and 42 weeks, cerebral blood velocities increased with increasing gestational age [46]. Premature and/or very low birth weight (VLBW) infants may have delayed development of this autoregulatory system, increasing the risk of abnormal flow and oxygenation of the brain during periods of hemodynamic instability. Premature infants have demonstrated a lower basal CBF [47] along with a compromised ability to regulate blood flow in the face of hemodynamic instability [48].

Delay in brain maturation may occur as a consequence of decreased oxygen and nutrient delivery in utero. In neonates with complex CHD, the delayed maturation of the brain, in conjunction with lower than expected postnatal CBF, may also lead to impaired autoregulation increasing the risk for brain injury during the pre-operative, intraoperative and post-operative period [49–51]. Regulation of blood flow during the transitional period is particularly challenging for neonates with either d-TGA or HLHS. In d-TGA, cerebral autoregulation may be limited by low arterial  $\text{PaO}_2$  (20–30 mm Hg range) particularly if there is an inadequate mixing at the atrial level [41]. In HLHS, the right ventricle provides flow to the pulmonary and systemic circulations with cerebral blood flow dependent on retrograde flow across the aortic

isthmus from the ductus arteriosus. As pulmonary vascular resistance falls in the first hours of life, there is a concomitant increase in pulmonary blood flow and physiological adaptations to maintain systemic perfusion may be inadequate in the setting of a single ventricle, potentially overwhelming the cerebral autoregulatory response. A delicate balance exists between pulmonary, cerebral and systemic perfusion. High oxygen saturations in HLHS patients, reflective of significant increases in pulmonary blood flow, may result in steal from the cerebral and systemic circulation if the vascular autoregulatory system is unable to compensate or overall cardiac output is limited. Prenatally, HLHS fetuses compensate by decreasing resistance as reflected by Doppler evidence of increasing diastolic flow in the MCA [33–35]. Whether this regulatory capacity has a threshold capacity or whether the ability to regulate CBF postnatally is influenced by the ability to regulate in utero remains to be answered. During the transitional period, those fetuses with the most significant changes in MCA flow may also be more susceptible to hemodynamic perturbations during transition. These patients may have a decrease autoregulatory capacity resulting in inadequate cerebral perfusion with changes in pulmonary vascular resistance and/or systemic blood pressure. Increasing understanding about the physiological changes that occur during this period will lead to improvement in management strategies to optimize CBF.

## 9. Magnetic resonance imaging identifies delayed brain development before surgery in CHD

Disordered fetal circulation places the brain at risk for disrupted growth and development during the third trimester. High resolution and advanced magnetic resonance imaging (MRI) techniques allow quantitative measurement of brain development. MR spectroscopic imaging (MRSI) and diffusion tensor imaging (DTI) assess brain metabolism and microstructure respectively. Proton MRSI can be used to measure N-acetylaspartate (NAA) [52]. NAA is found predominantly in neurons (cell body and axon), so that decreases and increases in NAA reflect neuronal metabolic integrity [52]. NAA increases consistently with development, providing a brain metabolic ‘growth chart’ [53]. Diffusion tensor imaging (DTI) provides a sensitive measure of regional brain microstructural development. DTI characterizes the three-dimensional spatial movement or diffusion of water in each voxel of the MR image [54]. With increasing brain maturation, brain water content diminishes and developing neuronal microstructure and myelination increasingly restrict proton diffusion resulting in a consistent decrease in average diffusivity ( $D_{av}$ ) over time in gray and white matter regions [54]. Using MRSI and DTI, brain metabolism and microstructure were compared between term newborns with CHD prior to heart surgery and normal controls [51]. Relative to the normal control newborns, newborns with CHD had 10% lower N-acetylaspartate/choline ratios and 4.5% higher  $D_{av}$ . Comparing these data to values obtained from normal fetuses, [54] suggests that term newborns with CHD have a delay in brain development of approximately one month, equivalent to an infant born prematurely at 34–36 weeks.

This delay in brain development has been assessed at a macroscopic level. Using an observational, semi-quantitative MRI metric developed and validated by Childs [55] termed Total Maturation Score (TMS), Licht et al. evaluated brain maturation in 42 full-term (average GA=38.9±1.1 weeks) infants born with CHD prior to surgery [50]. The TMS metric assesses 4 areas of brain development including 1) degree of myelination, 2) degree of cortical folding, 3) the radiographic presence or absence of germinal matrix in the anterior and posterior horns of the lateral ventricles and 4) the presence and number of migrating bands of glial cells. The study revealed symmetric delays in brain development across all four areas assessed, for an average TMS appropriate for infants born at 35 weeks of gestation. Thus the finding of a delay of 4 to 5 weeks in brain maturation is in strong agreement with the findings of Miller et al. who demonstrated evidence of biochemical delay of a similar magnitude in the white matter of these

same infants [51]. This finding is consistent across institutions and studies [49,56,57] and it is also consistent with the experimental data.

Reproducing the fetal environment for infants with CHD, Back et al. demonstrated that the maturation of pre-myelinating OL could be artificially arrested in mice pups reared in a hypoxic environment [23]. These hypoxic conditions gave rise to mice with ventriculomegaly and hypomyelination. The hypomyelination occurred in regions of brain depleted of pre-myelinating OLs, but did not show evidence of axonal loss or inflammatory infiltrate. The findings suggest that chronic hypoxia disrupted both the progress of OL differentiation and consequently the progression of myelination, an effect that was prevented by caffeine treatment. Importantly, despite excluding patients with perinatal distress or asphyxia, Licht et al. found evidence of hypoxic–ischemic brain injury (PVL) in >20% (9/42) of infants with severe CHD before surgery [50]. The areas of the affected white matter (Fig. 5) are homologous to the periventricular areas rich in pre-myelinating OLs in a fetal ovine model for PVL [58].

Thus, for infants with severe CHD, brain development is delayed both micro- and macro-structurally such that concentration of vulnerable pre-myelinating OL persists to term birth. Failure of nutrient and oxygen delivery during late gestation, transition from fetal to neonatal blood flow or post natal/pre-surgical care, results in white matter ischemia in the areas of brain (periventricular white matter) where these pre-myelinating OL endure. Delayed brain development may underlay the surprising preponderance of injury to periventricular white matter in term newborns with congenital heart disease. Periventricular white matter injury, and it's most severe form periventricular leukomalacia, are most commonly observed in prematurely born infants [59,60]. In support of this hypothesis, a low brain maturity score was associated with a higher risk of acquired brain injury in newborns with congenital heart disease [49]. Other risk factors for acquired brain injury include perioperative hypoxemia and hypotension [57,61–64]. These perioperative insults may represent the proximate cause of brain injury. However, individual susceptibility to these insults is influenced by the substrate of delayed brain development. An exhaustive consideration of risk factors for acquired injury is beyond the scope of this article.

## 10. Summary

Increasing data suggest that brain maturation and development is impaired in neonates with complex congenital heart defects. The delays in development arise from failures in brain oxygen and nutrient delivery unique to each form of congenital heart disease, with examples of deficient content (d-TGA) [24] or abnormalities in blood flow (HLHS) [33,35]. Delayed fetal brain maturation and development in utero appears to begin in the 3rd trimester of gestation and is consistent with postnatal data demonstrating smaller head circumferences and structurally immature brains in term gestation neonates with CHD compared to normal term neonates. Underlying the gross structural immaturity of the brain are delays in cellular maturation. The maturation of OL has been closely associated with an increased risk for hypoxic and oxidative injury to the white matter, which is seen commonly in neonates with CHD both before and after surgery. Evidence suggests that brain immaturity is the leading risk factor for PVL in neonates with complex CHD both before and after surgery [49]. Understanding cerebral blood flow regulation during fetal development, transition to neonatal circulation, pre-operative instrumentation and during post-operative recovery will be central to neuroprotective studies in the future.

## References

1. Rosenthal GL. Patterns of prenatal growth among infants with cardiovascular malformations: possible fetal hemodynamic effects. *Am J Epidemiol* 1996;143(5):505–13. [PubMed: 8610666]

2. Shillingford AJ, Ittenbach RF, Marino BS, Rychik J, Clancy RR, Spray TL, et al. Aortic morphometry and microcephaly in hypoplastic left heart syndrome. *Cardiol Young* 2007;17(2):189–95. [PubMed: 17338838]
3. Srivastava D. Making or breaking the heart: from lineage determination to morphogenesis. *Cell* 2006;126(6):1037–48. [PubMed: 16990131]
4. Francis F, Meyer G, Fallet-Bianco C, Moreno S, Kappeler C, Socorro AC, et al. Human disorders of cortical development: from past to present. *Eur J Neurosci* 2006;23 (4):877–93. [PubMed: 16519653]
5. Hoch RV, Rubenstein JL, Pleasure S. Genes and signaling events that establish regional patterning of the mammalian forebrain. *Semin Cell Dev Biol* 2009;20(4):378–86. [PubMed: 19560042]
6. Howard BM, Zhicheng M, Filipovic R, Moore AR, Antic SD, Zecevic N. Radial glia cells in the developing human brain. *Neuroscientist* 2008;14(5):459–73. [PubMed: 18467668]
7. Bayatti N, Moss JA, Sun L, Ambrose P, Ward JF, Lindsay S, et al. A molecular neuroanatomical study of the developing human neocortex from 8 to 17 postconceptional weeks revealing the early differentiation of the subplate and subventricular zone. *Cereb Cortex* 2008;18(7):1536–48. [PubMed: 17965125]
8. Kostovic I, Vasung L. Insights from in vitro fetal magnetic resonance imaging of cerebral development. *Semin Perinatol* 2009;33(4):220–33. [PubMed: 19631083]
9. Mrzljak L, Kostovic I, Uylings HB, Van Eden CG. Prenatal development of neurons in the human prefrontal cortex I. A qualitative Golgi study. *J Comp Neurol* 1988;271 (3):355–86. [PubMed: 2454966]
10. McQuillen PS, Ferriero DM. Perinatal subplate neuron injury: implications for cortical development and plasticity. *Brain Pathol* 2005;15(3):250–60. [PubMed: 16196392]
11. Kostovic I, Rakic P. Developmental history of the transient subplate zone in the visual and somatosensory cortex of the macaque monkey and human brain. *J Comp Neurol* 1990;297(3):441–70. [PubMed: 2398142]
12. Kostovic I, Rakic P. Development of prestriate visual projections in the monkey and human fetal cerebrum revealed by transient cholinesterase staining. *J Neurosci* 1984;4(1):25–42. [PubMed: 6693940]
13. Hevner RF. Development of connections in the human visual system during fetal mid-gestation: a DiI-tracing study. *J Neuropathol Exp Neurol* 2000;59(5):385–92. [PubMed: 10888368]
14. Sur M, Rubenstein JL. Patterning and plasticity of the cerebral cortex. *Science* 2005;310(5749):805–10. [PubMed: 16272112]
15. Torborg CL, Hansen KA, Feller MB. High frequency, synchronized bursting drives eye-specific segregation of retinogeniculate projections. *Nat Neurosci* 2005;8(1):72–8. [PubMed: 15608630]
16. Horton JC, Hocking DR. An adult-like pattern of ocular dominance columns in striate cortex of newborn monkeys prior to visual experience. *J Neurosci* 1996;16 (5):1791–807. [PubMed: 8774447]
17. Rakic P. Prenatal genesis of connections subserving ocular dominance in the rhesus monkey. *Nature* 1976;261(5560):467–71. [PubMed: 819835]
18. Garel C, Chantrel E, Elmaleh M, Brisse H, Sebag G. Fetal MRI: normal gestational landmarks for cerebral biometry, gyration and myelination. *Childs Nerv Syst* 2003;19(7–8):422–5. [PubMed: 12879340]
19. Paus T, Collins DL, Evans AC, Leonard G, Pike B, Zijdenbos A. Maturation of white matter in the human brain: a review of magnetic resonance studies. *Brain Res Bull* 2001;54(3):255–66. [PubMed: 11287130]
20. Back SA, Luo NL, Borenstein NS, Levine JM, Volpe JJ, Kinney HC. Late oligodendrocyte progenitors coincide with the developmental window of vulnerability for human perinatal white matter injury. *J Neurosci* 2001;21(4):1302–12. [PubMed: 11160401]
21. Back SA, Riddle A, McClure MM. Maturation-dependent vulnerability of perinatal white matter in premature birth. *Stroke* 2007;38(2 Suppl):724–30. [PubMed: 17261726]
22. Craig A, Ling Luo N, Beardsley DJ, Wingate-Pearse N, Walker DW, Hohimer AR, et al. Quantitative analysis of perinatal rodent oligodendrocyte lineage progression and its correlation with human. *Exp Neurol* 2003;181(2):231–40. [PubMed: 12781996]

23. Back SA, Craig A, Luo NL, Ren J, Akundi RS, Ribeiro I, et al. Protective effects of caffeine on chronic hypoxia-induced perinatal white matter injury. *Ann Neurol* 2006;60(6):696–705. [PubMed: 17044013]
24. Rudolph AM. Aortopulmonary transposition in the fetus: speculation on pathophysiology and therapy. *Pediatr Res* 2007;61(3):375–80. [PubMed: 17314701]
25. Degani S. Fetal cerebrovascular circulation: a review of prenatal ultrasound assessment. *Gynecol Obstet Invest* 2008;66(3):184–96. [PubMed: 18607112]
26. Greisen G. Effect of cerebral blood flow and cerebrovascular autoregulation on the distribution, type and extent of cerebral injury. *Brain Pathol* 1992;2(3):223–8. [PubMed: 1343837]
27. Groenenberg IA, Wladimiroff JW, Hop WC. Fetal cardiac and peripheral arterial flow velocity waveforms in intrauterine growth retardation. *Circulation* 1989;80 (6):1711–7. [PubMed: 2598433]
28. Abuhamad A, Falkensammer P, Reichartseder F, Zhao Y. Automated retrieval of standard diagnostic fetal cardiac ultrasound planes in the second trimester of pregnancy: a prospective evaluation of software. *Ultrasound Obstet Gynecol* 2008;31(1):30–6. [PubMed: 18098347]
29. Arduini D, Rizzo G. Normal values of Pulsatility Index from fetal vessels: a cross-sectional study on 1556 healthy fetuses. *J Perinat Med* 1990;18(3):165–72. [PubMed: 2200862]
30. Mari G, Deter RL. Middle cerebral artery flow velocity waveforms in normal and small-for-gestational-age fetuses. *Am J Obstet Gynecol* 1992;166(4):1262–70. [PubMed: 1566783]
31. Gramellini D, Folli MC, Raboni S, Vadora E, Merialdi A. Cerebral–umbilical Doppler ratio as a predictor of adverse perinatal outcome. *Obstet Gynecol* 1992;79(3):416–20. [PubMed: 1738525]
32. Degani S, Shapiro I, Lewinsky RM, Degani S, Lewinsky RM, Shapiro I. Doppler studies of fetal cerebral blood flow. *Ultrasound Obstet Gynecol* 1994;4(2):158–65. [PubMed: 12797213]
33. Donofrio MT, Bremer YA, Schieken RM, Gennings C, Morton LD, Eidem BW, et al. Autoregulation of cerebral blood flow in fetuses with congenital heart disease: the brain sparing effect. *Pediatr Cardiol* 2003;24(5):436–43. [PubMed: 14627309]
34. Jouannic JM, Benachi A, Bonnet D, Fermont L, Le Bidois J, Dumez Y, et al. Middle cerebral artery Doppler in fetuses with transposition of the great arteries. *Ultrasound Obstet Gynecol* 2002;20(2):122–4. [PubMed: 12153661]
35. Kaltman JR, Di H, Tian Z, Rychik J. Impact of congenital heart disease on cerebrovascular blood flow dynamics in the fetus. *Ultrasound Obstet Gynecol* 2005;25(1):32–6. [PubMed: 15593334]
36. McElhinney DB, Benson CB, Brown DW, Wilkins-Haug LE, Marshall AC, Zaccagnini L, et al. Cerebral blood flow characteristics and biometry in fetuses undergoing prenatal intervention for aortic stenosis with evolving hypoplastic left heart syndrome. *Ultrasound Med Biol* 2010;36(1):29–37. [PubMed: 19931971]
37. Szwast A, Tian Z, McCann M, Donaghue D, Rychik J. Right ventricular performance in the fetus with hypoplastic left heart syndrome. *Ann Thorac Surg* 2009;87(4):1214–9. [PubMed: 19324154]
38. Bassan H, Gauvreau K, Newburger JW, Tsuji M, Limperopoulos C, Soul JS, et al. Identification of pressure passive cerebral perfusion and its mediators after cardiac surgery. *Pediatr Res* 2005;57(1):35–41. [PubMed: 15531739]
39. Hinton RB, Andelfinger G, Sekar P, Hinton AC, Gendron RL, Michelfelder EC, et al. Prenatal head growth and white matter injury in hypoplastic left heart syndrome. *Pediatr Res* 2008;64(4):364–9. [PubMed: 18552707]
40. Limperopoulos C, Tworetzky W, McElhinney DB, Newburger JW, Brown DW, Robertson RL Jr, et al. Brain volume and metabolism in fetuses with congenital heart disease: evaluation with quantitative magnetic resonance imaging and spectroscopy. *Circulation* 2010;121(1):26–33. [PubMed: 20026783]
41. Artman, M.; Mahony, L.; Teitel, DF. *Neonatal Cardiology*. San Francisco: McGraw-Hill; 2002. Perinatal cardiovascular adaptations; p. 39-51.
42. Noori S, Stavroudis TA, Seri I. Systemic and cerebral hemodynamics during the transitional period after premature birth. *Clin Perinatol* 2009;36(4):723–36. v. [PubMed: 19944832]
43. Roche-Labarbe N, Carp SA, Surova A, Patel M, Boas DA, Grant PE, et al. Noninvasive optical measures of CBV, StO(2), CBF index, and rCMRO(2) in human premature neonates' brains in the first six weeks of life. *Hum Brain Mapp* 31(3):341–52. [PubMed: 19650140]

44. Pellicer A, Valverde E, Gaya F, Quero J, Cabanas F. Postnatal adaptation of brain circulation in preterm infants. *Pediatr Neurol* 2001;24(2):103–9. [PubMed: 11275458]
45. Kehrler M, Blumenstock G, Ehehalt S, Goelz R, Poets C, Schoning M. Development of cerebral blood flow volume in preterm neonates during the first two weeks of life. *Pediatr Res* 2005;58(5):927–30. [PubMed: 16183816]
46. Kehrler M, Krageloh-Mann I, Goelz R, Schoning M. The development of cerebral perfusion in healthy preterm and term neonates. *Neuropediatrics* 2003;34(6):281–6. [PubMed: 14681752]
47. Yoxall CW, Weindling AM. Measurement of cerebral oxygen consumption in the human neonate using near infrared spectroscopy: cerebral oxygen consumption increases with advancing gestational age. *Pediatr Res* 1998;44(3):283–90. [PubMed: 9727702]
48. Limperopoulos C, Gauvreau KK, O'Leary H, Moore M, Bassan H, Eichenwald EC, et al. Cerebral hemodynamic changes during intensive care of preterm infants. *Pediatrics* 2008;122(5):e1006–13. [PubMed: 18931348]
49. Andropoulos DB, Hunter JV, Nelson DP, Stayer SA, Stark AR, McKenzie ED, et al. Brain immaturity is associated with brain injury before and after neonatal cardiac surgery with high-flow bypass and cerebral oxygenation monitoring. *J Thorac Cardiovasc Surg* 2010;139(3):543–56. [PubMed: 19909994]
50. Licht DJ, Shera DM, Clancy RR, Wernovsky G, Montenegro LM, Nicolson SC, et al. Brain maturation is delayed in infants with complex congenital heart defects. *J Thorac Cardiovasc Surg* 2009;137(3):529–36. [PubMed: 19258059]
51. Miller SP, McQuillen PS, Hamrick S, Xu D, Glidden DV, Charlton N, et al. Abnormal brain development in newborns with congenital heart disease. *N Engl J Med* 2007;357(19):1928–38. [PubMed: 17989385]
52. Novotny E, Ashwal S, Shevell M. Proton magnetic resonance spectroscopy: an emerging technology in pediatric neurology research. *Pediatr Res* 1998;44(1):1–10. [PubMed: 9667363]
53. Kreis R, Hofmann L, Kuhlmann B, Boesch C, Bossi E, Huppi PS. Brain metabolite composition during early human brain development as measured by quantitative in vivo 1H magnetic resonance spectroscopy. *Magn Reson Med* 2002;48(6):949–58. [PubMed: 12465103]
54. Glenn OA, Quiroz EM, Berman JI, Studholme C, Xu D. Diffusion-weighted imaging in fetuses with unilateral cortical malformations and callosal agenesis. *AJNR Am J Neuroradiol*. 2009
55. Childs AM, Ramenghi LA, Cornette L, Tanner SF, Arthur RJ, Martinez D, et al. Cerebral maturation in premature infants: quantitative assessment using MR imaging. *AJNR Am J Neuroradiol* 2001;22(8):1577–82. [PubMed: 11559510]
56. Tavani F, Mahle WT, Zimmerman RA, Galli KK, Nicolson SC, Gaynor JW, et al. An MRI study of neurological injury before and after congenital heart surgery. *Circulation* 2002;106(90121):I–109–14.
57. McQuillen PS, Barkovich AJ, Hamrick SE, Perez M, Ward P, Glidden DV, et al. Temporal and anatomic risk profile of brain injury with neonatal repair of congenital heart defects. *Stroke* 2007;38(2 Suppl):736–41. [PubMed: 17261728]
58. Riddle A, Luo NL, Manese M, Beardsley DJ, Green L, Rorvik DA, et al. Spatial heterogeneity in oligodendrocyte lineage maturation and not cerebral blood flow predicts fetal ovine periventricular white matter injury. *J Neurosci* 2006;26(11):3045–55. [PubMed: 16540583]
59. Miller SP, Cozzio CC, Goldstein RB, Ferriero DM, Partridge JC, Vigneron DB, et al. Comparing the diagnosis of white matter injury in premature newborns with serial MR imaging and transfontanel ultrasonography findings. *AJNR Am J Neuroradiol* 2003;24(8):1661–9. [PubMed: 13679289]
60. Woodward LJ, Anderson PJ, Austin NC, Howard K, Inder TE. Neonatal MRI to predict neurodevelopmental outcomes in preterm infants. *N Engl J Med* 2006;355(7):685–94. [PubMed: 16914704]
61. Dent CL, Spaeth JP, Jones BV, Schwartz SM, Glauser TA, Hallinan B, et al. Brain magnetic resonance imaging abnormalities after the Norwood procedure using regional cerebral perfusion. *J Thorac Cardiovasc Surg* 2006;131(1):190–7. [PubMed: 16399311]
62. Hoffman GM, Mussatto KA, Brosig CL, Ghanayem NS, Musa N, Fedderly RT, et al. Systemic venous oxygen saturation after the Norwood procedure and childhood neurodevelopmental outcome. *J Thorac Cardiovasc Surg* 2005;130(4):1094–100. [PubMed: 16214525]

63. Petit CJ, Rome JJ, Wernovsky G, Mason SE, Shera DM, Nicolson SC, et al. Preoperative brain injury in transposition of the great arteries is associated with oxygenation and time to surgery, not balloon atrial septostomy. *Circulation* 2009;119(5):709–16. [PubMed: 19171858]
64. Soul JS, Robertson RL, Wypij D, Bellinger DC, Visconti KJ, du Plessis AJ, et al. Subtle hemorrhagic brain injury is associated with neurodevelopmental impairment in infants with repaired congenital heart disease. *J Thorac Cardiovasc Surg* 2009;138 (2):374–81. [PubMed: 19619781]

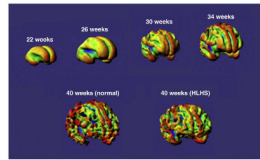


**Fig. 1.**

Summary of brain growth and curvature across development. T1-weighted MRIs were selected from fetuses (22, 26 weeks), premature infants (30, 34 weeks) and term newborns with and without congenital heart disease (hypoplastic left heart disease, HLHS). White matter volumes were reconstructed from manually segmented images. Curvature is represented in the color scale from concave (blue-green) to convex (yellow-red) and demonstrates onset and development of gyri and sulci. Brain volume and curvature are delayed in the term newborn with HLHS.

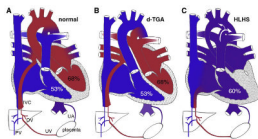


**Fig. 2.**

Normal fetal circulation and changes with congenital heart disease course of blood flow in a late gestation fetus with normal heart anatomy (A), d-transposition of the great arteries (B) and hypoplastic left heart syndrome due to aortic atresia (C). Deoxygenated blood (blue-purple) flows to the placenta through the umbilical artery (UA) where gas exchange takes place. Blood with higher oxygen content (red) returns through the umbilical vein (UV) and ductus venosus (DV) to the inferior vena cava (IVC). The more highly saturated blood forms a stream in the IVC, which is preferentially directed across the foramen ovale into the left ventricle in the normal fetus and with d-TGA. Estimated hemoglobin oxygen saturation in percent is shown for each ventricle. Blood flow to the fetal lungs is limited by elevated pulmonary vascular resistance. In the fetus with d-TGA, the aorta arises from the right ventricle such that the brain receives less oxygenated blood, while the higher saturated blood is directed to the descending aorta through the ductus arteriosus. In HLHS, reduced or absent left ventricular ejection results in elevated left atrial pressure, limiting or reversing flow at the foramen and resulting in complete mixing of desaturated and well saturated blood in the right atrium and ventricle. Blood flow to the head and neck may occur in a retrograde fashion from the ductus arteriosus across the aortic isthmus.

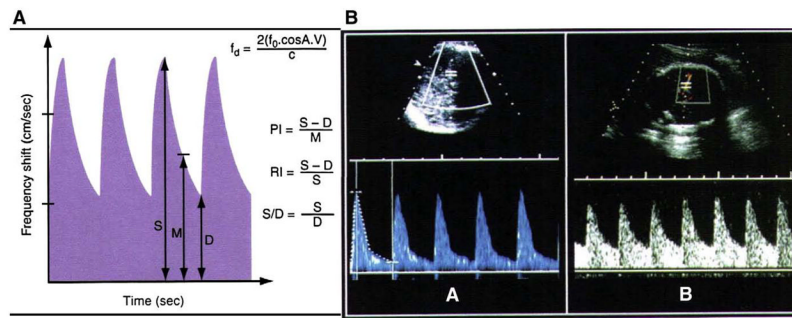


**Fig. 3.** A. Diagram for calculating pulsatility index (PI) and resistivity index (RI). B. Figure demonstrating middle cerebral artery measurements in a normal fetus (A) and a fetus with HLHS (B). Note the increase in the end-diastolic velocity. (Adapted from *Ultrasonography in Obstetrics and Gynecology* 5th Ed. Elsevier press).

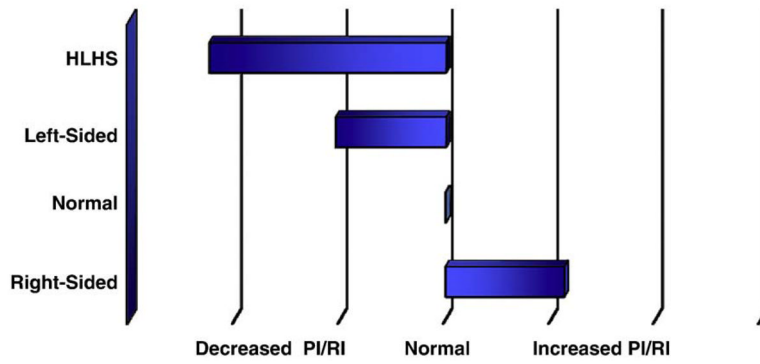


**Fig. 4.** Graphic representation of differences in relative fetal cerebrovascular resistance (X-axis) measured by Doppler ultrasound for hypoplastic left heart syndrome (HLHS) and heart lesions with right-sided or left-sided ventricle outflow track obstruction compared to normal.

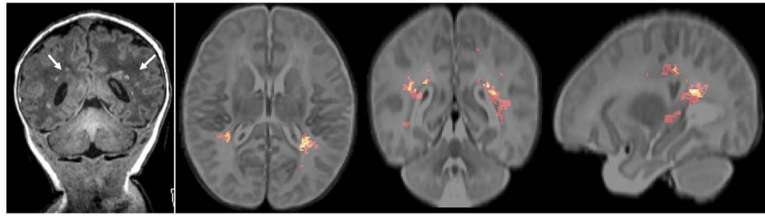


**Fig. 5.**

Typical distribution of periventricular leukomalacia (PVL) lesions. Far left frame — coronal T1 MRI demonstrating PVL lesions (white arrows). Right images (axial, coronal and sagittal) — manually traced periventricular white matter injury lesions (color areas; yellow — highest probability, red — lower probability) from 9 pre-surgical patients with either HLHS or TGA. The tracings are overlaid on a brain atlas composed of a composite of 42T2 volumetric brain MRIs (33 with HLHS and 19 TGA).